

Monte Carlo Study of the Critical Behavior of Pure and Site-Diluted Ising Ferro- and Ferrimagnets

P. Braun¹ and M. Fähnle¹

Received February 17, 1988; revision received March 28, 1988

Monte Carlo simulations are performed for pure and site-diluted Ising ferro- and ferrimagnets on a simple cubic lattice with up to 40^3 sites and with impurity concentration x . For the diluted ferromagnet ($x=0.2$) the exponent $\beta = 0.392 \pm 0.03$ is definitely larger than the pure model value of $\beta = 0.304 \pm 0.03$. In contrast, for ferrimagnetic systems ($x=0, 0.1, 0.2$) the β values appear to be independent of x and within the error limits consistent with the value for the pure ferromagnet, possibly because the width of the asymptotic random critical regime (or of the crossover regime) is even smaller than in the case of ferromagnets.

KEY WORDS: Critical phenomena; disordered spin systems; Ising model; Monte Carlo simulation.

1. INTRODUCTION

The second-order phase transition from the ferromagnetic state to the paramagnetic state of an isotropic pure ferromagnet at the critical temperature T_c is characterized by two independent critical exponents, for instance, the exponent γ of the zero-field susceptibility $\chi(T, H=0)$, $\chi \sim t^{-\gamma}$, and the exponent β of the spontaneous magnetization $M(T, H=0)$, $M \sim t^\beta$, with $t = |(T - T_c)/T_c|$. All other critical exponents describing the critical behavior of various thermodynamic quantities, for example, the exponent α of the zero-field specific heat $c(T, H=0)$, $c \sim t^{-\alpha}$, are related to the two exponents considered as the independent ones by scaling relations. In the language of renormalization theory,^(1,2) the critical behavior of such a

¹ Institut für Physik, Max-Planck-Institut für Metallforschung, 7000 Stuttgart 80, Federal Republic of Germany.

system is determined by one (stable) fixed point with two relevant parameters.

Outside the asymptotic critical regime the temperature dependence of the thermodynamic quantities is more complicated, and there is a wide transition regime from the critical behavior to the high-temperature behavior.⁽³⁾ To characterize the temperature dependence outside the asymptotic critical regime, Kouvel and Fisher⁽⁴⁾ have introduced temperature-dependent quantities,

$$\gamma(T) = (T - T_c) \chi d\chi^{-1}/dT \quad (1)$$

$$\beta(T) = (T_c - T) M dM^{-1}/dT = -(T_c - T) M^{-1} dM/dT \quad (2)$$

These quantities are constructed in such a way that they approach the critical exponents γ and β for $T \rightarrow T_c$ and the values $\gamma(T \rightarrow \infty) = 1$ (mean-field value) and $\beta(T \rightarrow 0) = 0$ (according to the third law of thermodynamics). As an example, Fig. 1 exhibits the temperature dependence of $\gamma(T)$ and $\beta(T)$ for the ferromagnetic model. The quantity $\gamma(T)$ decreases monotonically^(3,5) with increasing temperature for all known isotropic pure ferromagnets with short-range exchange interactions.

Introduction of spatial disorder into the system (for instance, by diluting with nonmagnetic atoms of concentration x) generates a more complicated situation. Because the parameter space of the renormalization transformation now is larger, the occurrence of one or more additional fixed points is expected. In the following we consider only the possibility of one additional physical fixed point; conceivable cases include: (1) the critical behavior is still determined by the stable one of the fixed points only; (2) the critical behavior is determined by a crossover from an unstable fixed point to the stable one (describing the behavior for $T \rightarrow T_c$). In both cases the stable fixed point may be (a) the original fixed point of the pure system ($x = 0$) with pure exponent values, or (b) a random fixed

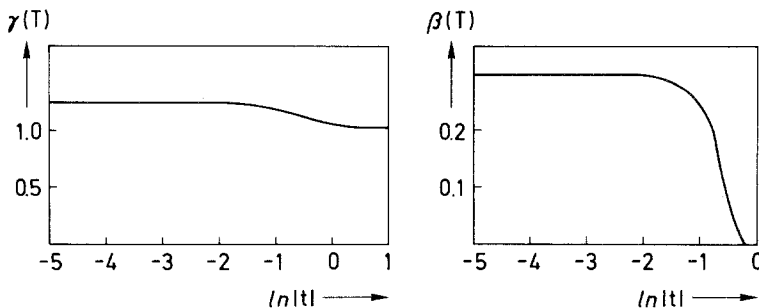


Fig. 1. Schematic representation of $\gamma(T)$ and $\beta(T)$ for an isotropic homogeneous ferromagnet with short-range exchange interactions.

point, with exponent values different from those of the pure fixed point and depending or not depending on x .

Figure 2 represents qualitatively the possible behavior of $\gamma(T)$ and $\beta(T)$ for disordered systems. It should be noted that these are only schematic plots and that the details should not be taken too literally (for instance, the crossover may be extended over more decades). If the crossover takes place rapidly and at temperatures very close to T_c , it is fully developed in the critical regime (solid lines in Fig. 2). Then there are two temperature ranges for which $\gamma(T)$ and $\beta(T)$ exhibit constant values,

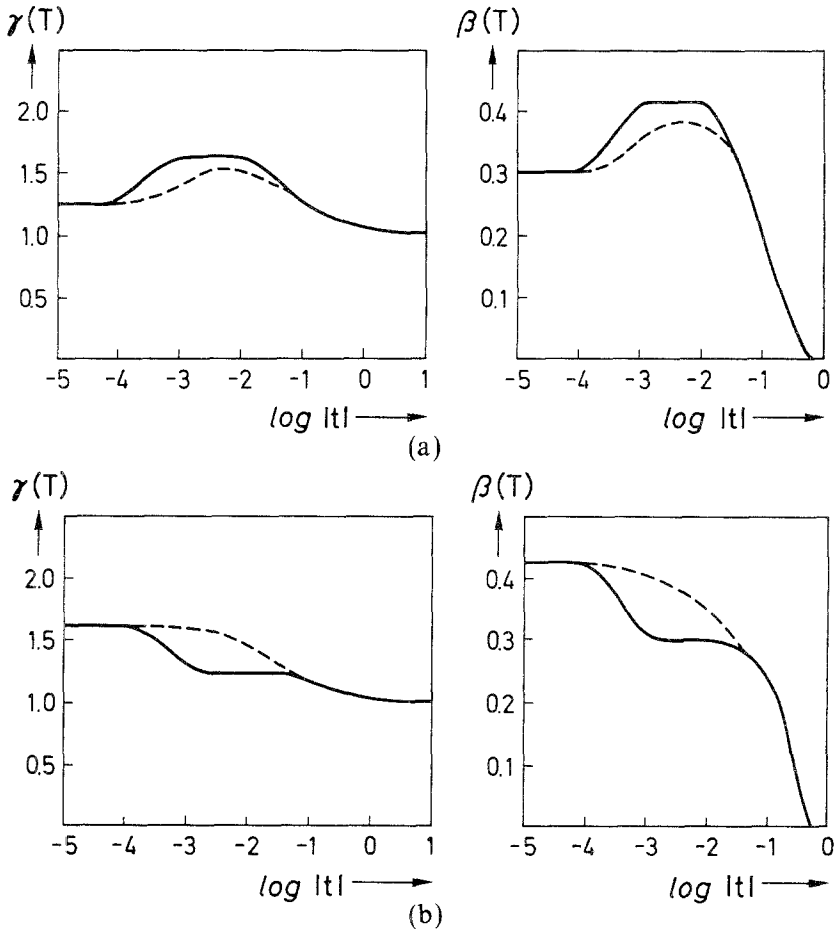


Fig. 2. Schematic representation of $\gamma(T)$ and $\beta(T)$ for a crossover between two fixed points, which is (—) fully developed or (- -) not fully developed in the critical regime. The exponent values for the unstable fixed point may be (a) larger or (b) smaller than the values for the stable fixed point. Note that the plots do not represent an adequate description of $\gamma(T)$ outside the critical regime (see text).

respectively, corresponding to the two fixed points. The exponent values of the unstable fixed point may be larger (Fig. 2a) or smaller (Fig. 2b) than those of the stable fixed point. In this case the crossover is described by scaling functions, which may be calculated by renormalization theory. Alternatively, the crossover regime may be extended, and the crossover possibly is not fully developed in the critical temperature range (dashed lines in Figs. 2). Then $\gamma(T)$ and $\beta(T)$ may not be described by scaling functions up to the maxima in Fig. 2a, for instance, and it is not guaranteed that a renormalization calculation going to temperatures outside the critical regime yields reasonable results. If the maxima of $\gamma(T)$ and $\beta(T)$ occur far outside the critical regime, then it no longer makes sense to argue that the thermodynamic behavior at these temperatures is determined by the unstable fixed point.

Theoretically, the best known conjecture for disordered systems is the Harris criterion, which was derived by Harris⁽⁶⁾ from heuristic arguments and was confirmed later by various renormalization calculations.⁽⁷⁻⁹⁾ It states that for weak disorder the pure fixed point remains stable if the specific heat exponent α of the pure system is negative, as for the $d=3$ Heisenberg model. In contrast, the transition is modified for positive α , as for the pure $d=3$ Ising model, and renormalization calculations have shown⁽⁷⁻¹²⁾ that in this case a new stable random fixed point appears. For weak disorder the exponent values corresponding to the random fixed point were determined by renormalization calculations,⁽¹⁰⁻¹²⁾ yielding values independent of x . It is expected^(13,14) that the random behavior is only developed in a very small asymptotic temperature range, whereas a large part of the critical regime is dominated by the crossover from the pure Ising model exponents to the random exponents (case 2b, Fig. 2b). Thereby the crossover possibly is very slow, so that the asymptotic random behavior is never really approached experimentally and some average effective exponent is observed.

A special renormalization treatment by Sobotta and Wagner^(15,16) for arbitrary concentration x (not necessarily weak disorder) also conceives the critical behavior of random spin systems as a crossover from an unstable to a stable fixed point. For Heisenberg systems the stable fixed point is the pure one, and for Ising systems it is a different one, but with exponent values not essentially different from the homogeneous ones (we denote it as a "homogeneous-type" fixed point in the following). The unstable fixed point exhibits (Fisher-renormalized) critical exponents identical to the spherical exponents in three dimensions, independent of the order parameter dimension n . The crossover between the two fixed points is fully developed for systems close to the percolation concentration, i.e., the main part of the critical regime is then determined by the spherical

exponent values (similar to Fig. 2a, solid lines), whereas for a smaller concentration of nonmagnetic atoms the experiments yield concentration-dependent effective (i.e., average) exponents. According to ref. 16, the asymptotic critical regime with homogeneous-type exponents is extremely small for all concentrations ($|t| < 10^{-8}$). In this theory, the stable fixed point is always the homogeneous-type fixed point (our case 2a), whereas in the renormalization calculations for weakly disordered Ising systems⁽¹⁰⁻¹²⁾ the stable fixed point is the random one (case 2b).

The results from Monte Carlo simulations are also not conclusive so far. A finite-size scaling analysis for small, site-diluted, simple cubic Ising ferromagnets⁽¹⁷⁾ was consistent with pure exponent values. This might correspond to our case 1a, or to case 2b with a very small asymptotic random regime not accessed by the simulations for small systems. Indeed, Monte Carlo simulations for large Ising ferromagnets with weak dilution revealed⁽¹⁸⁾ β values increasing continuously with increasing concentration x of nonmagnetic atoms. This might correspond to case 1b. Alternatively, taking the results of both simulations^(17,18) seriously suggests an interpretation according to case 2b: There is a small asymptotic critical regime corresponding to a random fixed point (not accessed by the simulations of Landau⁽¹⁷⁾), whereas the main part of the critical regime is dominated by the pure fixed point (Fig. 2b). Because even the large-system simulation of ref. 18 probably is not able to resolve the crossover, it yields effective, average exponent values for the considered temperature range which depend on concentration x because the width of the asymptotic regime or the width of the crossover regime may depend on x . Altogether, the Monte Carlo results suggest a flow from the unstable pure or homogeneous-type fixed point to the stable random fixed point, in agreement with the renormalization calculations of refs. 10-12 and in disagreement with refs. 15 and 16.

Outside the critical regime a nonmonotonic temperature dependence of $\gamma(T)$ was found by Monte Carlo simulations^(5,19) for diluted Ising ferromagnets, similar to the behavior of the dashed line in Fig. 2a. However, because the maximum of $\gamma(T)$ appears at rather high temperatures, $T = (1.1 - 2) T_c$, this behavior of $\gamma(T)$ (which is germane for a large class of disordered spin systems⁽⁵⁾) does not represent a critical phenomenon (see above discussion) and is not considered further in this paper. It is also not included in the schematical Fig. 2.

Experimentally the situation is also not clear. The site-diluted $d = 3$ Ising antiferromagnet $\text{Fe}_{1-x}\text{Zn}_x\text{F}_2$ revealed⁽²⁰⁾ exponent values consistent with those derived by ref. 12 for the random Ising fixed point in a rather large temperature range, $2 \times 10^{-3} \leq t \leq 10^{-1}$. This would correspond to our case 1b. However, it cannot be excluded that there is a very slow

crossover between two fixed points (case 2) in this temperature range, yielding an average exponent value which agrees accidentally with the theoretical random exponent value. Similarly, a study⁽¹⁴⁾ of the random Ising antiferromagnet $\text{Mn}_{0.864}\text{Zn}_{0.136}\text{F}_2$ for $5 \times 10^{-4} \leq t \leq 2 \times 10^{-2}$ yields a β value consistent with the prediction of a very slow crossover. For dysprosium aluminum garnet⁽²¹⁾ the perhaps effective β value increased from $\beta = 0.330 \pm 0.012$ for the pure system to $\beta = 0.35 \pm 0.01$ ($\beta = 0.385 \pm 0.025$) for the diluted model with 1 at % (5 at %) of non-magnetic yttrium. A detailed Mössbauer investigation⁽²²⁾ of the diluted Ising antiferromagnet $\text{Fe}_{1-x}\text{Zn}_x\text{F}_2$ revealed an abrupt crossover in the value of the β exponent from a concentration-independent value of $\beta = 0.36$ below a crossover temperature t_c to the pure exponent value of $\beta = 0.33$ above t_c (our case 2b, solid line in Fig. 2b).

In this paper we report on Monte Carlo simulations for pure and site-diluted Ising ferro and ferrimagnets. In Section 2.1 simulations for small ferromagnets are performed and analyzed by finite-size scaling theory, using the data collapsing method. It is shown that we cannot derive reliable exponent values from this method. In Section 2.2 the Monte Carlo simulation for large systems is evaluated and tested by repeating the calculations of ref. 18 for the ferromagnetic model. In Section 3 we extend the calculations to the pure and site-diluted Ising ferrimagnet ($S = \frac{1}{2}/1$). To our knowledge there is no Monte Carlo study of the ferrimagnetic transition at all (recent Monte Carlo studies^(23,24) consider a rather large temperature range and do not represent systematic investigations for the critical regime). For the homogeneous ferrimagnet it was conjectured⁽²⁵⁾ from results of high-temperature series expansions that its critical behavior is identical to the one of corresponding ferromagnets, in agreement with recent experimental results⁽²⁶⁾ for Heisenberg ferrimagnets. As in the case of ferromagnets, no influence of structural disorder on the critical behavior was found⁽²⁶⁾ in these systems. In the present Monte Carlo study for pure and diluted ($x = 0.1, 0.2$) Ising ferrimagnets the β values appear to be independent of x and within the error limits indeed consistent with the value for the pure ferromagnet. Conclusions are given in Section 4.

2. MONTE CARLO SIMULATIONS FOR THE ISING FERROMAGNETS

In this section we exemplify the Monte Carlo technique presently used by dealing with pure and site-diluted simple cubic Ising ferromagnets with N^3 sites and periodic boundary conditions. The model is described by the Hamiltonian

$$H = -J \sum_{\langle ij \rangle} S_i S_j \xi_i \xi_j \quad (3)$$

with $S_i = \pm 1$, $J > 0$, and summation over all nearest neighbor pairs $\langle ij \rangle$.

The occupation number ξ_i has the value 1 (0) if site i is occupied by a magnetic (nonmagnetic) atom. The diluted systems are generated by selecting randomly a site of the lattice and inserting at this site a magnetic atom, if it is not already occupied by a magnetic atom. Then the procedure is repeated until $(1-x)N^3$ magnetic atoms are distributed randomly on the lattice, and the nonmagnetic atoms are placed on the other sites.

We apply the usual Monte Carlo technique described, for instance, in refs. 17, 18, and 27–29. The program starts with a ferromagnetic or random initial spin configuration for the highest considered temperature, respectively, whereas it chooses as initial configuration for the next (lower) temperature the spin configuration after the last Monte Carlo step per spin for the preceding temperature. The first 10% of the Monte Carlo steps per spin are discarded for each temperature to allow for a relaxation to thermal equilibrium. In the following the temperature is normalized to $|J|/k_B$ and the magnetization values are normalized to the maximum values obtained for perfect magnetic order.

2.1. Simulations for Small Ising Ferromagnets

In this section we perform Monte Carlo simulations for small systems, $N = 6, 8, 10, 14,$ and 20 , and we analyze the data within the framework of finite-size scaling analysis by the data collapsing method.^(27–31) The calculations of Landau,^(27,31) for instance, qualitatively confirmed finite-size scaling for the two- and three-dimensional Ising model. The disadvantage is that it needs a fit of three parameters simultaneously, for instance, T_c , β , and the correlation exponent ν . Alternatively, one may assume a certain value, for example, for the exponent ν , insert a value of T_c obtained by another type of scaling plot, and obtain the β exponent by the data collapsing method. In any case, it turns out that a good data collapse may be obtained for several combinations of values T_c , β , and ν . It is the purpose of the present section to illustrate this disadvantage of the method, which has been outlined already in other papers (see, for instance, ref. 29). It will be shown explicitly that (contrary to a still widespread opinion) the method does not allow an adequate discussion of critical phenomena.

To calculate the thermodynamic averages, the spin configurations after each Monte Carlo step per spin have been used (after discarding the first 10%). For the pure model ($x = 0$), up to 2×10^4 (5×10^3) Monte Carlo steps per spin are performed for $N \leq 10$ ($N \geq 14$) and a ferromagnetic initial spin configuration is used for the highest temperature. Two runs are made for each temperature, one with a random selection of spins for the spin-flip trials and one which proceeds through the lattice in ordered sequence. For the random selection the statistical fluctuations of M , c , and χ are larger than for the ordered succession, and, for instance, the specific heat peak

occurs at slightly higher temperatures. The final results for $M(T)$ are obtained by averaging over the two runs. Close to T_c the thermodynamic quantities are calculated for temperatures in steps of $\Delta T = 0.01$. On this scale the temperature dependence of χ and c , respectively, exhibits a shoulder rather than a sharp peak near T_c , sometimes with several maxima resulting from statistical fluctuations. We define the pseudocritical temperature $T_c(N)$ of the finite system as the temperature for which the absolute maximum of c (of χ) occurs when proceeding through the lattice in ordered succession for the spin-flip trials. Because the location of the absolute maximum on the shoulder is determined by statistical fluctuations, there are statistical errors of $T_c(N)$, yielding the error bars in Fig. 3. Furthermore, there is a systematic error due to the uncertainty of whether $T_c(N)$ should be defined via the c or the χ maxima. As shown in Fig. 3, for finite systems these two maxima occur at different temperatures.⁽²⁷⁾ The critical temperature of the infinite system $T_c(\infty)$ is calculated from the finite-size scaling plot (Fig. 3), $T_c(N)$ versus $N^{-\lambda}$, with $\lambda = 1/\nu$. For the exponent ν of the correlation length we insert $\nu = 0.64$, in accordance with ref. 31. From the specific heat data we obtain for the pure model $T_c(\infty) = 4.503$ when including $T_c(6)$ or $T_c(\infty) = 4.486$ when omitting $T_c(6)$ from the scaling plot as in Fig. 3 [possibly $T_c(6)$ is already outside the asymptotic regime of the plot, as is also indicated in Figs. 4 and 5]. From the susceptibility data we find $T_c(\infty) = 4.513$ when omitting $T_c(6)$. The error for $T_c(\infty)$ due to the statistical fluctuations of $T_c(N)$ amount to $\Delta T_c = \pm 0.008$ for the c and χ data when omitting $T_c(6)$, whereas the above-discussed systematic error, i.e., the difference in $T_c(\infty)$ between the χ and c data, is $\Delta T_c = 0.027$.

The critical exponent β is determined from the finite-size scaling plot, $MN^{\beta/\nu}$ versus $tN^{1/\nu}$, with $t = |[T - T_c(\infty)]/T_c(\infty)|$. It depends very sensitively on the value inserted for $T_c(\infty)$. With $T_c(\infty) = 4.515$, for example, an optimum data collapse for the pure model is found (Fig. 4) for $\beta = 0.312$, a value obtained by Landau⁽³¹⁾ and close to $\beta = 0.325$ determined from renormalization theory.⁽³²⁾ For $T_c(\infty) = 4.50$, which is also within the error limit of $T_c(\infty)$, the scaling plot yields $\beta = 0.270$ (Fig. 5), whereas the plot for $T_c(\infty) = 4.50$ but $\beta = 0.312$ is much worse (Fig. 6). In Figs. 4–6 the circles according to the $N = 6$ data are included, but possibly they are already outside the asymptotic regime of the plot.

For the site-diluted ferromagnets we perform 5000 (2000, 1000) Monte Carlo steps per spin for $N = 6$ (10, 20) and $x = 0.2, 0.4$. Two different random initial spin configurations are used for the highest considered temperatures, respectively. Furthermore, two different structural configurations are considered for each concentration. Finally, the data for the thermodynamic quantities are averaged over all four runs. A random selection for the spin-flip trials is performed.

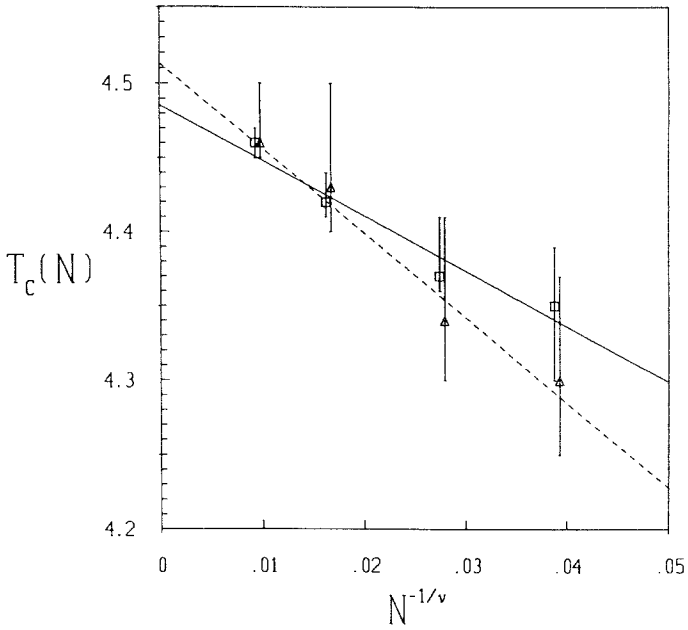


Fig. 3. Finite-size scaling plot for the pseudocritical temperatures of the pure Ising ferromagnet from the maxima in (\square) c and (\triangle) χ . The lines represent the corresponding least-mean-square fits. The two data sets are slightly shifted with respect to the $N^{-1/\nu}$ axis to avoid overlap of the error bars.

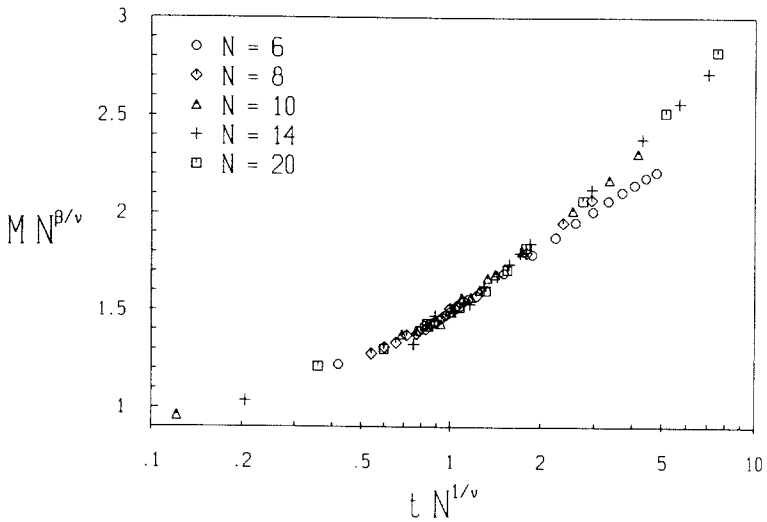


Fig. 4. Finite-size scaling plot for the magnetization of the pure model, with $T_c(\infty) = 4.515$ and $\beta = 0.312$.

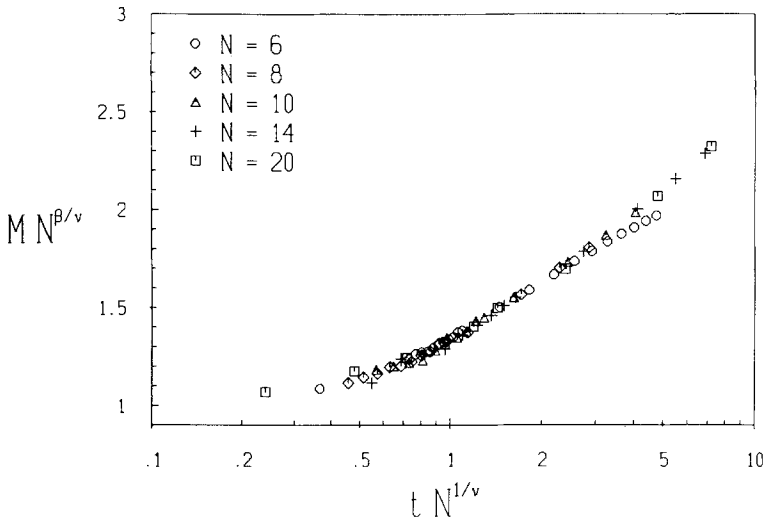


Fig. 5. Finite-size scaling plot for the magnetization of the pure model, with $T_c(\infty) = 4.50$ and $\beta = 0.27$.

The determination of the critical temperatures is now even less accurate than for the pure model. Due to the large statistical fluctuations, it is not reasonable to locate $T_c(N)$ with accuracy better than $\Delta T_c = \pm 0.1$. Furthermore, there is again a possible systematic error due to the difference in the peak location for the c and χ data. For example, for $x = 0.2$ (0.4) and

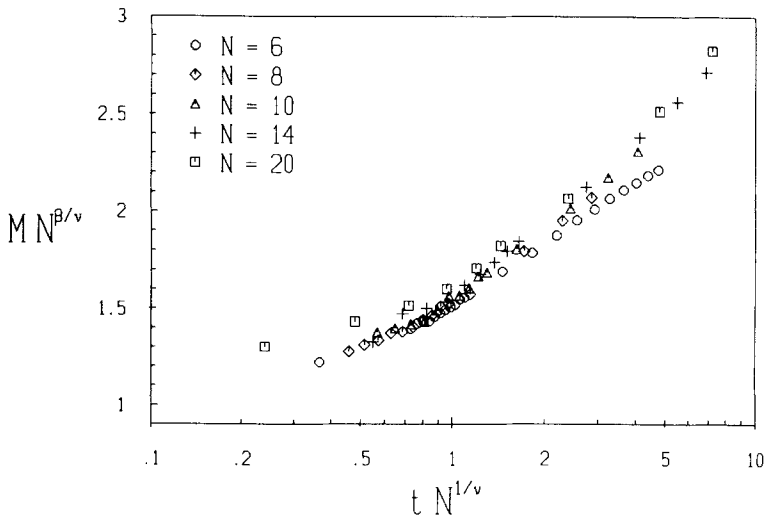


Fig. 6. Finite-size scaling plot for the magnetization of the pure model, with $T_c(\infty) = 4.50$ as in Fig. 5, but now with $\beta = 0.312$.

$N=20$ we obtain from the susceptibility peak $T_c(20)=3.5$ (2.4), whereas the specific heat peak yields $T_c(20)=3.3$ (2.3). As in the paper of Landau,⁽¹⁷⁾ the exponent β of the diluted model is determined from the slope of the plot $\ln M(N)$ versus $\ln |[T - T_c(N)]/T_c(N)|$, in fact for the largest system ($N=20$). As shown in Fig. 7, this yields for $x=0.2$ an exponent $\beta=0.30$ when inserting $T_c(20)=3.5$ from the χ peak, but $\beta=0.15$ for $T_c(20)=3.3$ from the c peak. Furthermore, it becomes obvious from Fig. 7 that due to the large uncertainty in the determination of $T_c(20)$, we possibly can never approach the asymptotic regime, but we probably obtain an average exponent value for a rather large temperature range.

Altogether, we conclude that we are not able to obtain reliable exponent values from our Monte Carlo simulations for small systems when applying the finite-size scaling analysis via the data collapsing method (or when analyzing by double-logarithmic plots). To extract accurate critical exponent values on the basis of Monte Carlo results for finite systems, more appropriate techniques must be used. A possible candidate is the cumulant method discussed, for example, by Binder,⁽²⁹⁾ Landau and Binder,⁽³³⁾ and Barber *et al.*⁽³⁴⁾ One advantage of this method is that T_c

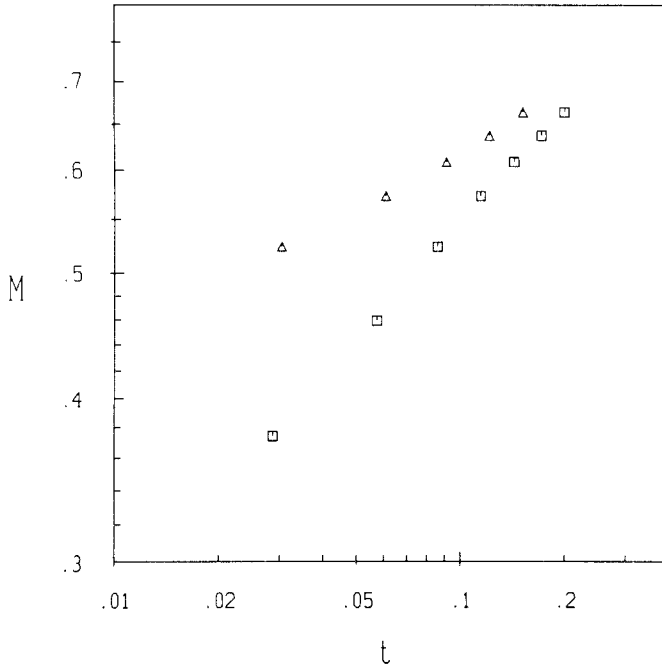


Fig. 7. The plot $\ln M$ versus $\ln t$ with $t = |[T - T_c(20)]/T_c(20)|$ for the diluted Ising ferromagnet ($x=0.2$) with (□) $T_c(20)=3.5$ and (△) $T_c(20)=3.3$.

and the exponent values are estimated in an independent way. Furthermore, one can take into account effects due to corrections to scaling in a reasonable way for $N > 24$ in the case of the three-dimensional Ising model.⁽³⁴⁾ In the following sections we use an alternative method, i.e., the simulation of large systems. This method allows for an analysis of the magnetization along the same line as commonly used for experimental data.^(26,35,36) As in the case of the cumulant method, the main advantage of this method is that the exponent value may be determined without any accurate knowledge of T_c . Furthermore, finite-size effects are less important from the very beginning.

2.2. Simulations for Large Ising Ferromagnets

In this section we perform simulations for large Ising ferromagnets ($N = 30$ for the pure model, $N = 40$ for the diluted model) similar to those described by ref. 18. The basic ideas are:

1. For very large systems the finite-size effect is rather small, and the thermodynamic behavior resembles very much that of an infinite system. We then can avoid the finite-size scaling plots and analyze the data for the biggest system size.⁽¹⁸⁾
2. Only small defect concentrations, $x \leq 0.2$, are considered. Then the detailed configuration has no observable influence on the thermodynamic quantities, and there is no need for a configurational average.
3. Combining the large lattice size with a large number of Monte Carlo steps per spin (10^4) yields rather small statistical fluctuations of the data, and there is no need for an average over several runs.
4. Only the magnetization data are analyzed, because they exhibit much smaller statistical fluctuations (Fig. 8) than those for c and χ (the latter quantities are related to thermodynamic fluctuations via the fluctuation-dissipation relation).
5. The crucial point in the analysis of the small-system data is the uncertainty in the determination of the critical temperature. Because for the present simulation of large systems the statistical fluctuations of the magnetization data are rather small, we can determine the exponent β by the so-called Kouvel-Fisher analysis,⁽⁴⁾ which does not require an accurate knowledge of T_c from the very beginning.

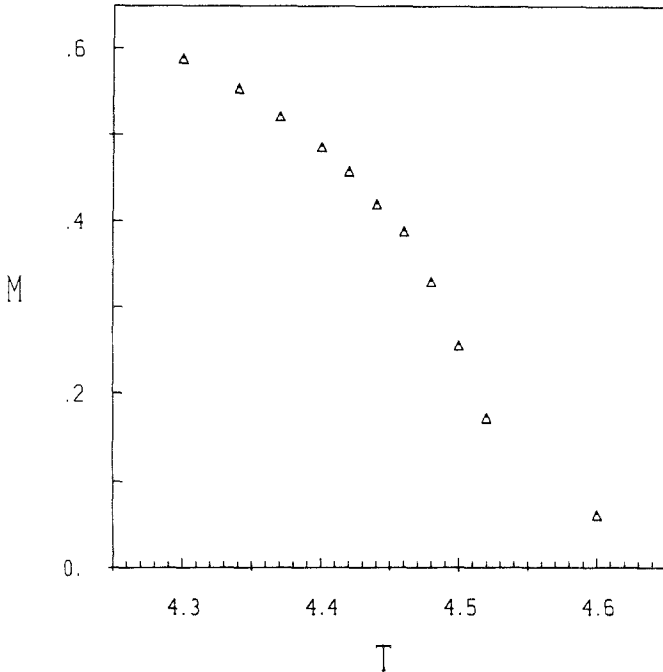


Fig. 8. Temperature dependence of M for the pure Ising ferromagnet for $N = 30$.

According to Eq. (2), the quantity $f = M(dM/dT)^{-1}$ is represented as function of T . For $T \rightarrow T_c$ the data are arranged around a straight line. The inverse slope of this line represents β , and the intersection with the T axis yields T_c (Fig. 9) (in Fig. 9 we omit the data for the three highest temperatures in Fig. 8 to avoid finite-size effects). Significant deviations from the straight line occur for the low-temperature data (in Fig. 9 only for the lowest one), indicating that the critical regime has been left. For the least mean square fit of the straight line we omit these data. Because in general the onset of deviations from the straight line is not precisely defined, the obtained values of β and T_c (and the corresponding error limits, see below) depend to some extent on our definition of the width of the critical regime. This problem is well known from the Kouvel-Fisher analysis of all experimental data.^(26,35,36) With those values for β and T_c we calculate the critical amplitude B according to $M = Bt^\beta$ by minimizing the quantity

$$S = \sum_i (M_i - Bt_i^\beta)^2 \tag{4}$$

Here M_i denotes the magnetization data at reduced temperatures $t_i = |[T_i - T_c(N)]/T_c(N)|$, with $N = 30$ (40) for the pure (diluted) model.

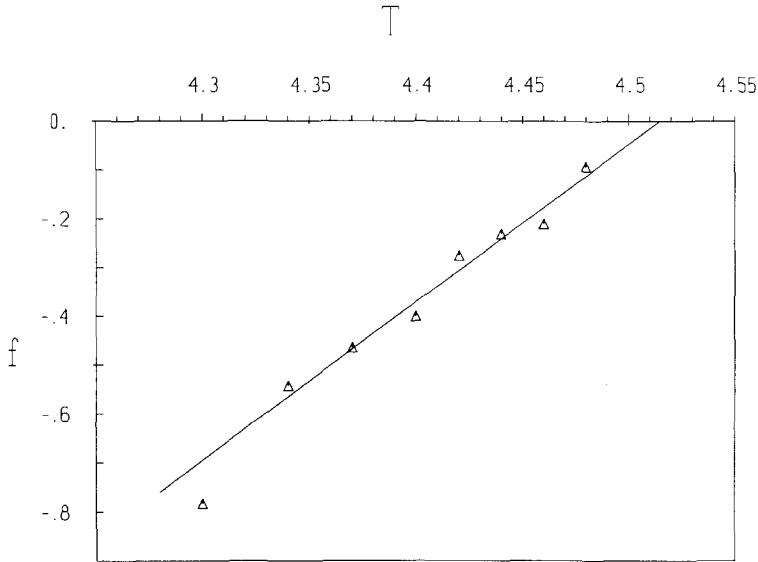


Fig. 9. Temperature dependence of $f = M(dM/dT)^{-1}$ as calculated from the data in Fig. 8. The straight line represents a least-mean-square fit.

Simulations are performed on this line, starting with a random initial spin configuration for the highest considered temperature. We proceed through the lattice in ordered succession for the spin-flip trials, and we calculate the thermodynamic averages by considering the spin configurations after four completed Monte Carlo steps per spin, respectively, to avoid correlations between successive measurements.⁽¹⁸⁾ The simulations are performed for temperature steps $\Delta T = 0.02$. We have used 10^4 Monte Carlo steps per spin. Because the largest relaxation mode τ near criticality scales according to $\tau \sim N^z$, where $z \approx 2$ is the dynamical exponent, it is reasonable to assume that the appropriate number of Monte Carlo steps also scales like N^2 . In his simulations for the diluted simple cubic Ising model Landau⁽¹⁷⁾ kept up to 5000 Monte Carlo steps per spin for $N \leq 30$. For our pure model ($N = 30$) we thus use about twice as many steps as Landau. Extrapolating from Landau's number for $N = 30$ to the appropriate number for $N = 40$ (as for our diluted model) yields 9000 steps, which exactly represents the number of steps we kept after discarding the first 10%. Our number of Monte Carlo steps per spin is also comparable to that used by ref. 18, namely 5000–11,000 steps for $N = 30, 40$. For the ferrimagnetic model (Section 3) we use an even larger number of Monte Carlo steps per spin, namely 1.5×10^4 .

For a calculation of the quantity dM/dT we represent the magnetization by a cubic spline, which does not smooth the fluctuations, but connects the data continuously and with continuous first and second derivative. As a result, small fluctuations in M induce fluctuations of $f = M(dM/dT)^{-1}$ and a scatter of the data in the $f(T)$ plot. This produces an error for the inverse slope of this line and its T -axis intersection, respectively. It should be noted, however, that those errors are not identical with the errors for β and T_c due to the magnetization fluctuations. To obtain those latter error limits, one would have to calculate the propagation of the error in $M(T)$ to the error in $f(T)$. This, however, is impossible, because the spline procedure and the differentiation dM/dT relate the fluctuations in both plots in a very complicated and not obvious manner. The errors $\Delta\beta$ and ΔT_c from the $f(T)$ plot thus only represent estimates for the real errors for β and T_c . As discussed above, these error limits also depend to some extent on the definition of the width of the critical regime. The error limit for B is then estimated by minimizing S [Eq. (4)], thereby combining the upper (lower) value of β , i.e., $\beta + \Delta\beta$ ($\beta - \Delta\beta$), with the upper (lower) value of T_c , i.e., $T_c + \Delta T_c$ ($T_c - \Delta T_c$).

For the pure ferromagnetic Ising model we obtain $\beta = 0.304 \pm 0.03$, $T_c = 4.513 \pm 0.009$, and $B = 1.49 \pm 0.13$. For comparison, series expansions⁽³⁷⁾ yield $0.303 \leq \beta \leq 0.318$, $T_c = 4.5108$, and $B = 1.569 \pm 0.003$. The simulations of ref. 18 give $\beta = 0.30 \pm 0.02$, $T_c = 4.510 \pm 0.004$, and $B = 1.5 \pm 0.2$, and renormalization calculations find $\beta = 0.325 \pm 0.001$ ⁽³²⁾ and $T_c = 4.5115 \pm 0.0001$.⁽³⁸⁾ For the site-diluted model with $x = 0.2$ we obtain $\beta = 0.392 \pm 0.03$, $T_c = 3.513 \pm 0.007$, and $B = 1.78 \pm 0.14$, which compares to $\beta = 0.385 \pm 0.015$, $T_c = 3.510 \pm 0.003$, and $B = 1.76 \pm 0.1$ from ref. 18. Obviously the β value for the site-diluted model is definitely larger than the value for the pure model. A possible interpretation is given in Section 1.

It should be noted that it is impossible to perform a corresponding Kouvel-Fisher analysis for our susceptibility data, because the scatter in the data is still too large for this type of analysis. One may try to improve the statistics by increasing the number of Monte Carlo steps per spin. Apart from the fact that we do not have that much computer time, we doubt that an arbitrary increase of the number of Monte Carlo steps per spin necessarily improves the accuracy of the susceptibility data. For very long calculation times the entire lattice may be overturned several times, which affects the susceptibility data.⁽²⁷⁾ We therefore did not attempt to consider the susceptibility along a similar line as the magnetization.

3. MONTE CARLO SIMULATIONS FOR LARGE ISING FERRIMAGNETS

In this section we extend the calculations to pure and diluted Ising ferrimagnets on a simple cubic lattice (N^3 sites), described by the Hamiltonian

$$H = -J \sum_{i,m} S_i^A S_m^B \xi_i \xi_m \quad (5)$$

with $J < 0$. The sum runs over all spins $S_i^A = \pm 1/2$ on the A sublattice and over all nearest neighbors S_m^B (with values 0 or ± 1) of the spins S_i^A , respectively, on the B sublattice. The occupation number ξ_i , for instance, has the value of 1 (0) if site i is occupied by a magnetic (nonmagnetic) atom, and we distribute by the procedure described in Section 2 exactly $(1-x)N^3/2$ magnetic atoms randomly on each sublattice.

Earlier simulations of this model⁽²³⁾ have shown that, for instance, the susceptibility of the strongly diluted system with $N=14$ exhibits rather large statistical fluctuations, which could not be considerably reduced by increasing the number of Monte Carlo steps per spin. We therefore perform the following simulations for large systems ($N=30$ for the pure model, $N=40$ for the diluted model) and small disorder ($x=0.1, 0.2$), and we analyze only the magnetization data by the Kouvel-Fisher method, as described in Section 2.2. The exponent β is determined from the sublattice magnetizations M_A and M_B (except for the pure model)

$$M_A = \sum_i S_i^A \xi_i, \quad M_B = \sum_j S_j^B \xi_j \quad (6)$$

the magnetization M ,

$$M = M_A + M_B \quad (7)$$

and the staggered magnetization M_S ,

$$M_S = M_A - M_B \quad (8)$$

Within the error limits the β values obtained from these four quantities are expected to be equal, in accordance with the experimental results⁽³⁹⁾ for magnetite, Fe_3O_4 . In the following all magnetization data are normalized to the maximum possible staggered magnetization for perfect ferrimagnetic order.

The Monte Carlo procedure and the data analysis are along the same line as for large Ising ferromagnets (Section 2.2), with 1.5×10^4 Monte Carlo steps per spin for each temperature. As an example, Fig. 10 shows

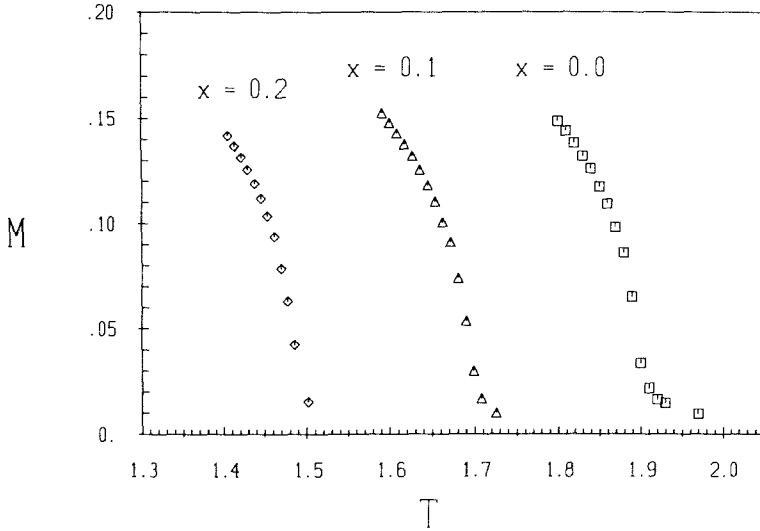


Fig. 10. Temperature dependence of the magnetization for the ferrimagnetic model with $x=0, 0.1, \text{ and } 0.2$.

the magnetization data. Because the scatter of the M data is even smaller than for the ferromagnetic model, the error limits for β , T_c , and B are also smaller.

Tables I–III represent the values of β , T_c , and B as determined from the Kouvel–Fisher plots for M_S , M , M_A , and M_B . The corresponding error estimates are determined from the $f(T)$ plot. Within the error limits the β values obtained from M_S , M , M_A , and M_B are roughly equal and consistent with the value of $\beta = 0.325 \pm 0.001$ as determined for the pure Ising ferromagnet from renormalization calculations⁽³²⁾ (we doubt that the small but seemingly systematic raise of the β values from the M data has

Table I. The β Values for the Pure and Diluted Ferrimagnet As Determined from M_S , M , M_A , and M_B

x	β			
	M_S	M	M_A	M_B
0.0	0.336 ± 0.015	0.353 ± 0.013	—	—
0.1	0.323 ± 0.024	0.341 ± 0.023	0.316 ± 0.024	0.326 ± 0.024
0.2	0.318 ± 0.014	0.336 ± 0.018	0.312 ± 0.014	0.322 ± 0.015

Table II. The Critical Temperature T_c for the Pure and Diluted Ferrimagnet As Determined from M_S , M , M_A , and M_B

x	T_c			
	M_S	M	M_A	M_B
0.0	1.900 ± 0.002	1.901 ± 0.002	—	—
0.1	1.693 ± 0.004	1.695 ± 0.003	1.693 ± 0.004	1.694 ± 0.004
0.2	1.484 ± 0.002	1.485 ± 0.002	1.483 ± 0.002	1.484 ± 0.002

any physical meaning). For the pure ferrimagnet we obtain $T_c = 1.900 \pm 0.002$, which compares to $T_c = 1.92 \pm 0.04$ from high-temperature series expansions.⁽⁴⁰⁾ Furthermore, within the error limits we cannot detect an influence of dilution on the β value of ferrimagnetic systems, in contrast to the results for ferromagnetic systems. Possibly the width of the crossover regime is smaller than for diluted ferromagnets, so that it cannot be accessed even by our simulations for large systems.

4. CONCLUSIONS

In this paper we have reported on Monte Carlo simulations for pure and diluted Ising ferro- and ferrimagnets on a simple cubic lattice with N^3 sites and impurity concentration x . Due to the statistical error in the determination of the critical temperature T_c reliable exponent values could not be obtained by simulations of small systems ($N \leq 20$) with finite-size scaling analysis via the data collapsing method. Instead we have performed simulations for large systems (up to $N = 40$) with rather small statistical fluctuations of the magnetization data. This allows for a determination of the exponent β from a Kouvel–Fisher plot, which does not require the

Table III. The Critical Amplitude B for M_S , M , M_A , and M_B for the Pure and Diluted Ferrimagnet

x	B			
	M_S	M	M_A	M_B
0.0	1.52 ± 0.06	0.42 ± 0.015	—	—
0.1	1.41 ± 0.08	0.39 ± 0.03	0.51 ± 0.03	0.90 ± 0.05
0.2	1.34 ± 0.05	0.38 ± 0.02	0.49 ± 0.01	0.86 ± 0.04

knowledge of an accurate T_c value from the very beginning. For the diluted ferromagnet with $x=0.2$ a β value of 0.392 ± 0.03 was found, which is larger than the value of $\beta=0.304 \pm 0.03$ for the pure model. This proves that the phase transition of the diluted Ising ferromagnet is not determined only by the pure Ising fixed point. The β value for the pure Ising ferrimagnet is consistent with that of the pure Ising ferromagnet, and the T_c value agrees with the critical temperature found by Schofield and Bowers⁽⁴⁰⁾ from high-temperature series expansions. Within the error limits no influence of dilution on the β value of ferrimagnets could be detected for $x=0.1$ and $x=0.2$, possibly because the width of the random asymptotic critical regime or of the crossover regime is even smaller than in the case of ferromagnets.

It is planned to speed up the Monte Carlo calculations by a multispin coding algorithm⁽⁴¹⁾ for simulations of even larger systems, and to attack the problem of diluted $d=3$ ferro- and ferrimagnets by means of a Monte Carlo renormalization calculation.⁽³⁸⁾

REFERENCES

1. S.-K. Ma, in *Modern Theory of Critical Phenomena* (Benjamin, Reading, Massachusetts, 1976).
2. A. Aharony, in *Phase Transitions and Critical Phenomena*, Vol. VI, C. Domb and M. S. Green, eds. (Academic Press, New York, 1976), pp. 357ff.
3. M. Fähnle and J. Souletie, *J. Phys. C* **17**:L469 (1984); *Phys. Rev. B* **32**:3328 (1985); *Phys. Stat. Sol. (b)* **138**:181 (1986).
4. J. S. Kouvel and M. E. Fisher, *Phys. Rev.* **136**:A1626 (1964).
5. M. Fähnle, *J. Mag. Mag. Mat.* **65**:1 (1987).
6. A. B. Harris, *J. Phys. C* **7**:1671 (1974).
7. U. Krey, *Phys. Lett. A* **51**:189 (1975).
8. T. C. Lubensky, in *Ill-Condensed Matter*, R. Balian, R. Maynard, and G. Toulouse, eds. (North-Holland, Amsterdam, 1979), pp. 408ff.
9. R. B. Stinchcombe, in *Phase Transitions and Critical Phenomena*, Vol. VII, C. Domb and J. L. Lebowitz, eds. (Academic Press, New York, 1983), pp. 152ff.
10. D. E. Khmel'nitskii, *Sov. Phys. JETP* **41**:981 (1976).
11. K. E. Newman and E. K. Riedel, *Phys. Rev. B* **25**:264 (1982).
12. G. Jug, *Phys. Rev. B* **27**:609 (1983).
13. S. Fishman and A. Aharony, *J. Phys. C* **12**:L729 (1977).
14. R. A. Dunlap and A. M. Gottlieb, *Phys. Rev. B* **23**:6106 (1981).
15. G. Sobotta and D. Wagner, *J. Phys. C* **11**:1467 (1978); *J. Mag. Mag. Mat.* **49**:77 (1985).
16. G. Sobotta and D. Wagner, *J. Mag. Mag. Mat.* **15-18**:257 (1980).
17. D. P. Landau, *Phys. Rev. B* **22**:2450 (1980).
18. A. Labarta, J. Marro, and J. Tejada, *Physica* **142B**:31 (1986); J. Marro, A. Labarta, and J. Tejada, *Phys. Rev. B* **34**:347 (1986).
19. M. Fähnle, *J. Mag. Mag. Mat.* **45**:279 (1984); *J. Phys. C* **18**:181 (1985).
20. R. J. Birgeneau, R. A. Cowley, G. Shirane, H. Yoshizawa, D. P. Belanger, A. R. King, and V. Jaccarino, *Phys. Rev. B* **27**:6747 (1983).

21. J. M. Hastings, L. M. Corliss, and W. Kunmann, *Phys. Rev. B* **31**:2902 (1985).
22. P. H. Barrett, *Phys. Rev. B* **34**:3513 (1986).
23. M. Fähnle and M. Haug, *Phys. Stat. Sol. (b)* **140**:569 (1987).
24. C. J. Tinsley, *Phil. Mag. B* **56**:351 (1987).
25. R. G. Bowers and B. Y. Yousif, *Phys. Lett. A* **96**:49 (1983).
26. M. Haug, M. Fähnle, H. Kronmüller, and F. Haberey, *Phys. Stat. Sol. (b)* **144**:353 (1987); *J. Mag. Mag. Mat.* **69**:163 (1987).
27. D. P. Landau, *Phys. Rev. B* **13**:2997 (1976).
28. K. Binder, in *Monte Carlo Methods in Statistical Physics*, K. Binder, ed. (Springer, Berlin, 1979), Chapter 1.
29. K. Binder, *J. Comp. Phys.* **59**:1 (1985).
30. M. N. Barber, in *Phase Transitions and Critical Phenomena*, Vol. VIII, C. Domb and J. L. Lebowitz, eds. (Academic Press, New York, 1983), pp. 146ff.
31. D. P. Landau, *Phys. Rev. B* **14**:255 (1976).
32. J. C. Le Guillou and J. Zinn-Justin, *Phys. Rev. Lett.* **39**:95 (1977); *Phys. Rev. B* **21**:3976 (1980).
33. D. P. Landau and K. Binder, *Phys. Rev. B* **31**:5946 (1985).
34. M. N. Barber, R. B. Pearson, D. Toussaint, and J. L. Richardson, *Phys. Rev. B* **32**:1720 (1985).
35. S. N. Kaul, *J. Mag. Mag. Mat.* **53**:5 (1985).
36. W.-U. Kellner, M. Fähnle, H. Kronmüller, and S. N. Kaul, *Phys. Stat. Sol. (b)* **144**:331 (1987).
37. C. Domb, in *Phase Transitions and Critical Phenomena*, Vol. III, C. Domb and M. S. Green, eds. (Academic Press, New York, 1974), pp. 357ff.
38. G. S. Pawley, R. H. Swendsen, D. J. Wallace, and K. G. Wilson, *Phys. Rev. B* **29**:4030 (1984).
39. O. Steinsvoll, *Physica Scripta* **26**:119 (1982); O. Steinsvoll and T. Riste, *J. Mag. Mag. Mat.* **14**:187 (1979).
40. S. L. Schofield and R. G. Bowers, *J. Phys. A* **14**:2163 (1981).
41. G. O. Williams and M. H. Kalos, *J. Stat. Phys.* **37**:283 (1984).